Surface and nonlocal effects on response of linear and nonlinear NEMS devices

Prashant N.Kambali[a], Nikhil V. S.[a], Ashok Kumar Pandey[a,*]

[a] *Department of Mechanical and Aerospace Engineering, Indian Institute of Technology Hyderabad, Kandi, Sangaredyy, Telangana-502285, India.*

This is the accepted form of the paper on 3 November 2016 in Applied Mathematical Modelling, Eisevier. The copyright belongs to Elsevier ©and the paper can be downloded from http://dx.doi.org/10.1016/j.apm.2016.10.063

Abstract

Nonlocal and surface effects become important for nanoscale devices. To model these effects on frequency response of linear and nonlinear nanobeam subjected to electrostatic excitation, we use Eringen's nonlocal elastic theory and surface elastic theory proposed by Gurtin and Murdoch to modify the governing equation. Subsequently, we apply Galerkin's method with exact mode shape including nonlocal and surface effects to get static and dynamic modal equations. After validating the procedure with the available results, we analyze the variation of pull-in voltage and frequency resonance by varying surface and nonlocal parameters. To do frequency analysis of nonlinear system, we solve nonlinear dynamic equation using the method of multiple scale. We found that the frequency response of nonlinear system reduces for fixed excitation as the surface and nonlocal effects increase. Also, we found that the nature of nonlinearity can be tuned from hardening to softening by increasing the nonlocal effects.

Keywords: Surface effects, Nonlocal effects, Pull-in Voltage, Linear and nonlinear frequency

*Corresponding author

Email address: ashok@iith.ac.in (Ashok Kumar Pandey)

1. Introduction

Microelectromechanical systems (MEMS) and nanoelectromechanical systems (NEMS) have been explored widely in the design of resonant sensors and actuators in various fields [1, 2, 3, 4]. For the design and safe operation of the MEMS/NEMS devices, pull-in instability analysis is also very important. Pull-in voltage is defined as a critical voltage at which the physical equilibrium point loses its stability. Pull-in instability can be static or dynamic. Static pull-in is defined as critical dc voltage required to produce maximum stable displacement from initial equilibrium position. Dynamic pull-in is defined as critical ac voltage required for the collapse of the elastic structure toward the substrate at low dc voltage below static pull-in [5, 6]. The performance of resonant sensors is mostly characterized by the resonance frequency and the damping [7]. To improve their sensitivity, the size of such devices have been reduced to submicron or nanoscale. Due to high sensitivity of such devices, accurate computation of the resonance frequency and their frequency response are essential from the design prospective. An accurate computation of resonance frequency requires correct modeling of mechanical effects such as the bending, stretching, rotation, and shearing, etc., in nanobeams. To compute the frequencies in nanoscale structure, there are mainly two techniques, one is based on atomistic simulation [8, 9, 10], and another is based on the continuum method [11, 12]. While the atomistic simulation becomes computationally expensive, traditional continuum method gives inaccurate results due to the negligence of small scale and surface effects, respectively. Therefore, correct modeling of scale and surface effect is important to capture the mechanical effects accurately. In this paper, we discuss about the scale and surface effects on the linear and nonlinear frequency response of an electrostatically excited fixed fixed beam.

The set of eigen circular frequencies of transversal vibrations of a beam is generally found by solving partial differential equation of transversal vibrations either by Euler-Bernaulli thoery or Timoshenko theory with or without nonlinear geometric effects. However, when the scale effect dominates, which

influences the material properties of nanoscale devices [13], it is generally modelled by Eringen's theory of nonlocal-elasticity [14, 15]. Nonlocal-elastic theory states that the stress at a point is not only the function of strain at that point but it also depends on the strains in whole volume [14]. Consequently, the terms in classical beam equations are modified to capture the nonlocal effects accordingly. Similarly, the surface effect, which becomes dominant as surface to volume ratio increases in submicron or nanoscale structure [16], is modeled based on the surface elasticity theory as proposed by Gurtin and Murdoch [17]. According to surface elastic theory, surface effect is defined as increase in surface to bulk energy ratio, due to high surface/volume ratio in nanoscale regime. The validity of surface elasticity theory is also validated with the experimental results in different cases [16, 18, 19]. Therefore, for analysing the frequency response of the submicron or nanoscale beams, the combined surface and nonlocal effects should be analyzed.

There have been many studies available in the literature that describe the modeling of surface and nonlocal effects, either separately or as a combined effect on the linear and nonlinear free vibration of the nanostructures. He *et al* [20] theoretically modeled the surface effects to study the free transverse vibrations of nanowires. Sheng *et al* [21] also investigated the surface effects on the free transverse vibrations of MEMS devices. Abbasion *et al* [22] considered the surface effects in analysing the free vibrations of microbeam based on Timoshenko theory. Gheshlaghi *et al* [23] and Hashemi *et al* [24] modelled the surface effects along with the geometric nonlinearity to compute the variation of nonlinear free transverse vibrations of nanobeams. Lu *et al* [25] performed size-dependent static and dynamic analysis of plate-like thin film structures by proposing a general thin plate theory including surface effects. Liu *et al* [26] presented a theoretical model which considers surface energy effects based on Gurtin-Murdoch continuum theory to analyze thick and thin nanoscale beams with an arbitrary cross section under different loading and boundary conditions. Hu *et al* [27] studied the buckling and free vibrations of nonlocal nanowires by including surface elasticity. Hu *et al* [28] also investigated slant edge cracked

effect on the free transverse vibrations of nanobeams considering the inherent relation between surface energy and mixed-mode crack propagations and surface effect. To model the nonlocal effects, Pradhan and Murmu [1] performed frequency analysis based on nonlocal elasticity for single wall carbon nanotube embedded in elastic media. While Wang *et al* [29] analyzed the free vibrations of beam using Timoshenko theory, Murmu *et al* [30] included it in analysing the transverse vibrations of two nanobeams systems. Later, Reddy [31] included the nonlocal effect in the nonlinear analysis of the bending of beams and plates. Ke *et al* [32] investigated nonlinear free transverse vibrations of the piezoelectric nanobeams including the nonlocal effect. Hu *et al* [33] demonstrated the scale effect on coupling of in-plane and out-of-plane modal frequencies in nanoresonators. In addition to the individual effects of surface and the nonlocal effects, some researchers carried out different studies to model both surface and nonlocal effects. Lee *et al* analyzed the combined effects of surface and nonlocal on transversal vibrations of beam using Timoshenko theory [34] and of non-uniform nanobeams using Euler-Bernaulli theory [35], respectively. Nazemnezhad *et al* [36] modeled the combined effect to investigate the variation of nonlinear free transverse vibrations of nanobeams. Recently, Malekzadeh *et al* [12] investigated surface and nonlocal effects on the nonlinear free transverse vibrations of non-uniform nanobeams. While most of the previous studies were focused on modeling the surface and nonlocal effects in the bending and nonlinear geometric terms, Ardito *et al* [37] investigated the free vibration of micromechanical resonators under the effect of nonlocal thermoelastic damping. Lei *et al* [38] also investigated the effect of nonlocal Kelvin-Voigt viscoelastic damping on the frequency of nonlocal Timoshenko beam. Based on the above studies, free vibration frequencies of the beam of submicron to nanoscale length are found to be sensitive to the surface and nonlocal effects. Recent research trend focus on the modeling of nonlocal and surface effects on the resonance frequency and the pull-in effect (a common phenomena in MEMS [39, 40, 41]) of electrostatically excited beam of submicron to nanoscale dimensions. Mousavi *et al* [42] and Yang *et al* [43] investigated the pull-in stability of nano switches

using nonlocal elasticity theory. Recently, Fakhrabadia *et al* [11] also modelled the nonlocal effect in the bending and the forcing term of the electrostatically actuated carbon nanotubes to study the pull-in effect. Pasharavesh *et al* [44] considered the nonlocal effect in the inertial and forcing term to investigate the transverse vibrations of nonlinear clamped-clamped and cantilever beam using approximate mode shapes. While they found that the resonance frequency of cantilever increases with increase in size, that of doubly-clamped beam reduces with size.

From the above literatures, it is found that the surface and nonlocal effects play an important role in the dynamic characteristics of nanobeams. However, there are hardly any literature that present the comprehensive modeling of combined surface and nonlocal effects on the frequency of linear and nonlinear system vibrations of electrostatically excited nanobeams at large bias voltage. In this paper, we obtain governing partial differential equation of nonlinear system by including the non-local effect in terms related with inertial, linear and nonlinear stiffness, bending, damping, and forcing term of electrostatically excited fixed-fixed nanobeam. To capture the surface effects, we also modify the linear and nonlinear stiffness terms in the governing equation. To do the static and dynamic analysis, we apply Galerkin's method with exact mode shape obtained by considering surface and nonlocal effects to get static as well as modal dynamic equations, respectively. The exact mode shape is derived considering nonlocal effects , the surface effects , initial tension following the procedure as found in [45] . Subsequently, we do static analysis to find the pull-in voltage with surface and nonlocal effects. After validating the pull-in voltage with the available results in the literature without considering nonlocal and surface effects, we do frequency analysis of linear and nonlinear system vibrations. To do the frequency analysis of nonlinear system vibrations, we apply the method of multiple scale (MMS) to obtain approximate solution. After validating the solution based on MMS with the numerical solution from the modal dynamic equation, we investigate the influence of surface and nonlocal effects on the nonlinear frequency response of the beam.

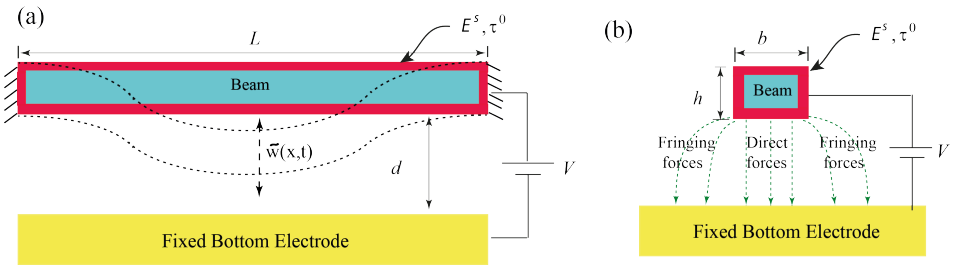

Figure 1: (a) Description of the transverse motion of a fixed-fixed beam with respect to the bottom electrode under the influence of electric voltage V. (b) Electric field lines showing the direct and fringing field effect along a section of electrostatically excited fixed-fixed beam. Here, E^s and τ^0 are elastic surface modulus and residual surface tension, respectively.

2. Governing partial differential equation of transversal vibrations of beam

In this section, we obtain the governing partial differential equation of transversal vibrations of a fixed-fixed beam subjected to electrostatic actuation using modified classical elastic theory by including nonlocal and surface effects, respectively. To obtain the governing equation, we consider a fixed-fixed homogeneous prismatic beam with rectangular cross section of length L, width b, thickness h which is separated from the bottom electrode by a distance of d, respectively, as shown in fig. 1(a). The beam is electrostatically excited by applying voltage $V = V_{\rm dc} + v(t)$, where $v(t) = V_{\rm ac}\cos(\Omega t)$ across the beam and bottom electrode.

(a) *Surface effect:* To capture the surface effect, the classical constitutive relation of the surface boundaries ($y = \pm b/2$; $z = \pm h/2$) as given by Gurtin and Murdoch [17] and also the classical constitutive relations for the internal material of the beam under large transverse deflection (-$b/2$< y< $b/2$; -$h/2$< z <$h/2$) can be expressed as:

$$\sigma^s = \tau^0 + E^s\epsilon_{\bar{x}\bar{x}}, \quad \sigma_{\bar{x}\bar{x}} = E\epsilon_{\bar{x}\bar{x}}, \quad \epsilon_{\bar{x}\bar{x}} = \frac{\partial\tilde{u}}{\partial\bar{x}} + \frac{1}{2}\left(\frac{\partial\tilde{w}}{\partial\bar{x}}\right)^2 - z\frac{\partial^2\tilde{w}}{\partial\bar{x}^2} \qquad (1)$$

where,τ^0 is the residual surface axial stress, E^s is the surface elastic modulus, $\tilde{u}$ and $\tilde{w}$ are the axial and transverse deflection, $\epsilon_{\bar{x}\bar{x}}$ is the effective axial strain under large bending condition, E is the Young's modulus of the

internal material of the beam. Assuming the neglgible axial deflection as compared to the transverse deflection, $\frac{\partial \bar{u}}{\partial \bar{x}} \to 0$. The stress resultants also containing the surface effects can be utilized to find the effective axial force and the moment as:

$$N_{\bar{x}\bar{x}} = \int_{-\frac{h}{2}}^{\frac{h}{2}} \sigma_{\bar{x}\bar{x}} b dz + \oint \sigma^s ds = (EA)_s \frac{1}{2}\Big(\frac{\partial \tilde{w}}{\partial \bar{x}}\Big)^2 + 2\tau^0(b+h) \tag{2}$$

$$M = \int_{-\frac{h}{2}}^{\frac{h}{2}} z\sigma_{\bar{x}\bar{x}} b dz + \oint z\sigma^s ds = (EI)_s \left[- \frac{\partial^2 \tilde{w}}{\partial \bar{x}^2} \right] \tag{3}$$

where, $A = bh$ is cross sectional area, $(EA)_s$ and $(EI)_s$ are the effective in-plane and flexural rigidities, respectively, and which can be written as [12]:

$$(EA)_s = EA + 2E^s(b+h) \qquad \text{and} \qquad (EI)_s = EI + E^s\left(\frac{h^3}{6} + \frac{bh^2}{2}\right) \tag{4}$$

(b) *Nonlocal effect:* In order to include the nonlocal effect, the relationship between the nonlocal stress, σ_{ij}^{nl}, and the local stress, σ_{ij}^{l}, is obtained by Eringen [14, 15], which is given by the following differential constitutive relation

$$\left(1 - \bar{\mu}\frac{\partial^2}{\partial \bar{x}^2}\right)\sigma_{ij}^{\text{nl}} = \sigma_{ij}^{l} \tag{5}$$

where,$\bar{\mu} = (e_0 a)^2$ is the nonlocal scale parameter, e_0 is the material constant, and a is the internal characteristic length. Using the stress relation from Eq. (5), the nonlocal axial tension and bending moments can be written as:

$$\left(1 - \bar{\mu}\frac{\partial^2}{\partial \bar{x}^2}\right)N_{\bar{x}\bar{x}}^{\text{nl}} = N_{\bar{x}\bar{x}}^{l} \tag{6}$$

$$M^{nl} - \bar{\mu}\frac{\partial^2 M^{nl}}{\partial \bar{x}^2} = M^{l} = EI\left[- \frac{\partial^2 \tilde{w}}{\partial \bar{x}^2} \right] \tag{7}$$

(c) *Governing equation:* Considering nonlocal effect in following terms, such as the unsteady inertia term [12], axial tension term [12], damping term [38] and the external forcing term [11], based on equivalent Eringen's model,

i.e., $\left(1-\bar{\mu}\frac{\partial^2}{\partial\bar{x}^2}\right)X^{\mathrm{nl}} = X^l$, where, X is variable, we can obtain a similar governing equation as described in [12]. Neglecting the in-plane deflection as compared to the transverse deflection, $\frac{\partial N^{\mathrm{nl}}_{\bar{x}\bar{x}}}{\partial\bar{x}} \to 0$, we get $N^{\mathrm{nl}}_{\bar{x}\bar{x}} = N^{l}_{\bar{x}\bar{x}}$ [12]. Finally, including the surface effect, nonlocal effect, and residual tension N_0, the equation of transverse vibration, $\tilde{w}$ can be written as

$$\left(1-\bar{\mu}\frac{\partial^2}{\partial\bar{x}^2}\right)\rho A\frac{\partial^2\tilde{w}}{\partial\bar{t}^2} + \frac{\partial^2}{\partial\bar{x}^2}\left[(EI)_s\frac{\partial^2\tilde{w}}{\partial\bar{x}^2}\right] - \left(1-\bar{\mu}\frac{\partial^2}{\partial\bar{x}^2}\right)\left[N^{\mathrm{nl}}_{\bar{x}\bar{x}}\frac{\partial^2\tilde{w}}{\partial\bar{x}^2}\right] + \left(1-\bar{\mu}\frac{\partial^2}{\partial\bar{x}^2}\right)C\frac{\partial\tilde{w}}{\partial\bar{t}} = \left(1-\bar{\mu}\frac{\partial^2}{\partial\bar{x}^2}\right)Q^e. \tag{8}$$

where,$\bar{\mu} = (e_0 a)^2$ is the nonlocal scale parameter, $N^{\mathrm{nl}}_{\bar{x}\bar{x}}$ is the resultant axial tension [12], $(EI)_s$ and $(EA)_s$ are the effective flexural and axial rigidities [12], Q^e is excitation force per unit length which is based on the assumption of parallel plate capacitor [39]. The expressions of these quantities are given by

$$N^{\mathrm{nl}}_{\bar{x}\bar{x}} = N_0 + \frac{1}{2}\left(\frac{\partial\tilde{w}}{\partial\bar{x}}\right)^2(EA)_s + 2\tau^0(b+h),$$

$$(EI)_s = EI + E^s\left(\frac{h^3}{6}+\frac{bh^2}{2}\right), \qquad (EA)_s = EA + 2E^s(b+h), \tag{9}$$

$$Q^e = \frac{\epsilon_0 b V^2}{2(d-\tilde{w})^2}\left[1+0.65\frac{(d-\tilde{w})}{b}\right] \tag{10}$$

where, τ^0 and E^s are residual surface tension and elastic surface modulus, ρ is density, $A = bh$ is cross sectional area, E is Young's modulus, $I = \frac{bh^3}{12}$ is axial moment of inertia of beam cross section for neutral axis of beam bending, N_0 is the pretention and C is damping constant. The force Q as mentioned in Eq. (10) consists of direct and fringing field effects as described in fig. 1(b). To obtain the generalized solution, we simplify the governing equation by substituting Eqs. (9) and (10) in Eq. (8) as

$$\begin{aligned}\rho A\tilde{w}_{\bar{t}\bar{t}} - \bar{\mu}\rho A\tilde{w}_{\bar{x}\bar{x}\bar{t}\bar{t}} + (EI)_s\tilde{w}_{\bar{x}\bar{x}\bar{x}\bar{x}} - N_0\tilde{w}_{\bar{x}\bar{x}} + \bar{\mu}N_0\tilde{w}_{\bar{x}\bar{x}\bar{x}\bar{x}} - \frac{1}{2}(EA)_s(\tilde{w}_{\bar{x}})^2\tilde{w}_{\bar{x}\bar{x}} \\ + \frac{1}{2}\bar{\mu}(EA)_s(\tilde{w}_{\bar{x}})^2\tilde{w}_{\bar{x}\bar{x}\bar{x}\bar{x}} - 2\tau^0(b+h)\tilde{w}_{\bar{x}\bar{x}} + 2\bar{\mu}\tau^0(b+h)\tilde{w}_{\bar{x}\bar{x}\bar{x}\bar{x}} + \bar{\mu}(EA)_s \\ \left[(\tilde{w}_{\bar{x}\bar{x}})^2 + \tilde{w}_{\bar{x}}\tilde{w}_{\bar{x}\bar{x}\bar{x}}\right]\tilde{w}_{\bar{x}\bar{x}} + C\tilde{w}_{\bar{t}} - \bar{\mu}C\tilde{w}_{\bar{x}\bar{x}\bar{t}} = Q^e(\tilde{w},\bar{t}) - \bar{\mu}Q^e_{\bar{x}\bar{x}}(\tilde{w},\bar{t}).\end{aligned} \tag{11}$$

To solve the above equation for fixed-fixed beam, we obtain the following boundary conditions

$$\tilde{w}(0,\bar{t}) = 0, \tilde{w}_{\bar{x}}(0,\bar{t}) = 0, \tilde{w}(L,\bar{t}) = 0, \tilde{w}_{\bar{x}}(L,\bar{t}) = 0. \tag{12}$$

(d) *Nondimensionalization:* To study the pull-in phenomena and response of nonlinear system of vibrations of fixed-fixed nanobeam with surface and nonlocal effcts under electrostatic actuation, we non-dimensionalize the above equations and boundary conditions with the following non-dimensional parameters $w = \frac{\tilde{w}}{d}$, $t = \bar{t}\omega_s$, $x = \frac{\bar{x}}{L}$, ${\omega_s}^2 = \frac{(EI)_s}{\rho A L^4}$, $\mu = \frac{\bar{\mu}}{L^2}$ as follow:

$$w_{tt} - \mu w_{xxtt} + w_{xxxx} - \alpha_1 w_{xx} + \alpha_2 w_{xxxx} - \beta_1 (w_x)^2 w_{xx} + \beta_2 (w_x)^2 w_{xxxx}$$
$$+\beta_3 \Big[(w_{xx})^2 + w_x w_{xxx} \Big] w_{xx} + k_1 w_t - k_2 w_{xxt} = \frac{f_{11} V^2}{(1-w)^2} - \frac{f_{12}(w_{xx}) V^2}{(1-w)^3}$$
$$- \frac{f_{13}(w_x)^2 V^2}{(1-w)^4} + \frac{f_{21} V^2}{(1-w)} - \frac{f_{22}(w_{xx}) V^2}{(1-w)^2} - \frac{f_{23}(w_x)^2 V^2}{(1-w)^3}, \tag{13}$$
$$w(0,t) = 0, w_x(0,t) = 0, w(1,t) = 0, w_x(1,t) = 0, \tag{14}$$

where,

$$\alpha_1 = [N_0 + 2\tau^0 (b+h)] \frac{L^2}{(EI)_s}, \quad \alpha_2 = \mu \alpha_1, \quad \beta_1 = \frac{1}{2} \frac{(EA)_s}{(EI)_s} d^2, \quad \beta_2 = \mu \beta_1,$$
$$\beta_3 = 2\beta_2, \quad k_1 = \frac{C}{\rho A \omega_s}, \quad k_2 = \mu k_1, \quad f_{11} = \frac{\epsilon_0 b L^4}{2 d^3 (EI)_s}, \quad f_{12} = 2\mu f_{11}$$
$$f_{13} = 6\mu f_{11}, \quad f_{21} = \frac{0.65 \epsilon_0 L^4}{2 d^2 (EI)_s}, \quad f_{22} = \mu f_{21}, \quad f_{23} = 2\mu f_{21}. \tag{15}$$

To do the static and dynamic analysis of the above equation, we assume transverse displacement $w(x,t)$ as a sum of static deflection z_s and dynamic component $z(x,t)$ as follow

$$w(x,t) = z_s(x) + z(x,t). \tag{16}$$

3. Static Analysis

In this section, we perform static analysis to study the effect of nonlocal and surface parameters on pull-in voltage under the combined effect of direct as well as fringing forces. The differential equation of static equilibrium governing

$z_s(x)$ is obtained by substituting Eq. (16) into Eq. (13), and subsequently setting the time derivative and dynamic displacement $z(x,t)$ equal to zero. Thus, the resulting equation for static deflection $z_s(x)$ can be written as:

$$\begin{aligned} z_{sxxxx} - \alpha_1 z_{sxx} + \alpha_2 z_{sxxxx} - \beta_1 (z_{sx})^2 z_{sxx} + \beta_2 (z_{sx})^2 z_{sxxxx} \\ + \beta_3 \Big[z_{sxx}^2 + z_{sx} z_{sxxx} \Big] z_{sxx} = \frac{f_{11} V_{dc}^2}{(1-z_s)^2} - \frac{f_{12}(z_{sxx}) V_{dc}^2}{(1-z_s)^3} \\ - \frac{f_{13}(z_{sx})^2 V_{dc}^2}{(1-z_s)^4} + \frac{f_{21} V_{dc}^2}{(1-z_s)} - \frac{f_{22}(z_{sxx}) V_{dc}^2}{(1-z_s)^2} - \frac{f_{23}(z_{sx})^2 V_{dc}^2}{(1-z_s)^3}. \end{aligned} \tag{17}$$

To solve the above equation, we assume the solution based on the single mode approximation as $z_s(x) = q\phi(x)$, where $\phi(x)$ is exact mode shape obtained by considering nonlocal effects, the surface effects, initial tension. It can be readily reduce to form of exact mode shape with nonlocal effects as mentioned in [45] by neglecting initial tension and surface effects. The form of characteristic equation and mode shape $\phi(x)$ for fixed-fixed beam which satisfy the appropriate boundary similar to [45] are given by

$$\begin{aligned} (e_0 a)^2 k_f k_e \sinh(k_e L) \sin(k_f L) + 2\cosh(k_e L)\cos(k_f L) - 2 = 0, \\ \phi(x) = \cosh(k_e x) - \cos(k_f x) - \frac{(k_e \sinh(k_e L) + k_f \sin(k_f L))}{k_e (\cosh k_e L - \cos k_f L)} \\ \times \left[\sinh(k_e x) - \frac{k_e}{k_f} \sin(k_f x) \right], \end{aligned} \tag{18}$$

where,

$$k_f = \lambda \sqrt{\frac{\sqrt{4 + ((e_0 a \lambda)^2 - (N/\lambda^2))^2} + ((e_0 a \lambda)^2 - (N/\lambda^2))}{2}},$$

$$k_e = \lambda \sqrt{\frac{\sqrt{4 + ((e_0 a \lambda)^2 - (N/\lambda^2))^2} - ((e_0 a \lambda)^2 - (N/\lambda^2))}{2}},$$

$$\lambda = \sqrt{\frac{\omega}{c_0}},\ c_0 = \sqrt{((EI)_s + (e_0 a)^2 N)/\rho A},\ N = N_0 + 2\tau_0(b+h).$$

For the first mode approximation, the eigenvalues of the clamped-clamped beam with nonlocal parameter $\frac{e_0 a}{L}$ and $N = 1.8054 \times 10^{-6}$ are given as

Substituting $z_s(x) = q\phi(x)$ into the governing Eq. (17) and then applying Galerkin method, the static equation can be rewritten as:

$$r_1 q + r_2 q^2 + r_3 q^3 + r_4 q^4 + r_5 q^5 + r_6 q^6 + r_7 q^7 = r_8 V_{dc}^2 - r_9 V_{dc}^2 q - r_{10} V_{dc}^2 q^2$$

Table 1: First mode eigenvalues of clamped-clamped beam with nonlocal parameter $\frac{e_0 a}{L}$ and for $N = 1.8054 \times 10^{-6}$

$\frac{e_0 a}{L}$	0	0.1	0.2	0.3	0.4	0.5	0.6	0.7	0.8
λL	4.73	4.594	4.276	3.918	3.592	3.315	3.084	2.889	2.725

$$-r_{11} V_{dc}^2 q^3 \tag{19}$$

where,

$$r_1 = \alpha_2 J_4 + J_4 - \alpha_1 J_5, \quad r_2 = 4\,\alpha_1 J_6 - 4\,J_9 - 4\,\alpha_2 J_9,$$
$$r_3 = -6\,\alpha_1 J_{11} + 6\,\alpha_2 J_{12} - \beta_1 J_{13} + \beta_2 J_{15} + 6\,J_{12} + \beta_3 J_{41} + \beta_3 J_{42},$$
$$r_4 = -4\,\alpha_2 J_{18} - 4\,\beta_2 J_{19} - 4\,J_{18} + 4\,\beta_1 J_{20} + 4\,\alpha_1 J_{22} - 4\beta_3 J_{43} - 4\beta_3 J_{44},$$
$$r_5 = \alpha_2 J_{23} - \alpha_1 J_{25} + 6\,\beta_2 J_{26} + J_{23} - 6\,\beta_1 J_{27} + 6\beta_3 J_{45} + 6\beta_3 J_{46},$$
$$r_6 = -4\,\beta_2 J_{28} + 4\,\beta_1 J_{29} - 4\beta_3 J_{47} - 4\beta_3 J_{48}, \quad r_7 = -\beta_1 J_{30} + \beta_2 J_{31}$$
$$+\beta_3 J_{49} + \beta_3 J_{50}, \quad r_8 = (f_{11} + f_{21})\,J_1, \quad r_9 = (f_{22} + f_{12})\,J_5 + (2\,f_{11} + 3\,f_{21})\,J_2,$$
$$r_{10} = -\,(f_{12} + 2\,f_{22})\,J_6 - (f_{11} + 3\,f_{21})\,J_8 + (f_{13} + f_{23})\,J_{10},$$
$$r_{11} = f_{21} J_{17} + f_{22} J_{11} - f_{23} J_{16}.$$

Since the static deflection of the beam approaches to infinity at the pull-in voltage, we get $\frac{dq}{dV} \to \infty$ or $\frac{dV}{dq} = 0$. After differentiating Eq. (19) w.r.t. q, and substituting $\frac{dV}{dq} = 0$, we get the expression of pull-in voltage which includes the nonlocal and surface effects as follow:

$$V_p = \Bigg(-\Big(r_9 + 2\,r_{10} q + 3\,r_{11} q^2\Big)\Big(r_1 + 2\,r_2 q + 3\,r_3 q^2 + 4\,r_4 q^3 + 5\,r_5 q^4 + 6\,r_6 q^5 + 7\,r_7 q^6\Big)\Bigg)^{1/2} \Big(r_9 + 2\,r_{10} q + 3\,r_{11} q^2\Big)^{-1} \tag{20}$$

where, q is the solution of equation which is obtained by substituting V_p into Eq. (19), J's are constants which are mentioned in appendix A.

3.1. Comparison and Validation

To validate the pull-in voltage with available expressions in the literature, we make the surface and nonlocal terms to zero, i.e, $\frac{e_0 a}{L} = 0, \tau^0 = 0, E^s = 0$

in Eq. (20). To compare the results, we first compare the formulas [41, 46, 47] which are based on approximate mode shape assumptions without considering geometric nonlinearity. Subsequently, we compare the results with the model [40] which is based on exact mode shape and also includes geometric nonlinearity.

- For comparison with the models based on approximate mode shapes, we take the dimensions and properties of a nanobeam [41] as mentioned in Table 2. On comparing the pull-in voltage obtained by substituting the surface and nonlocal terms (i.e. $\frac{e_0 a}{L} = 0, \tau^0 = 0, E^s = 0$) in Eq. (20), we get a lower value for the pull-in voltage as compared to that obtained from Chao *et al* [46], Fang *et al* [47] and Pandey[41] with percentage differences of 5.4%, 7.2% and 14%, respectively. Such differences are due to approximate mode shapes being used by Chao *et al* [46], Fang *et al* [47] and Pandey[41].

- To compare the model based on exact mode shape, we take the dimension and properties of beam [40] as mentioned in Table 3. When we compare the results obtained from Eq. (20) by substituting the surface and nonlocal terms (i.e. $\frac{e_0 a}{L} = 0, \tau^0 = 0, E^s = 0$) with that obtained from Nayfeh *et al* [40], we get a percentage difference of 8%. It is due to the fact that the results from Nayfeh *et al* [40] are based on summation of three or five mode shapes, however, in our model we approximate the transverse displacement by first mode approximation.

Based on the above comparisons, we validate our model to compute pull-in voltage including the surface as well as nonlocal effects.

4. Linear and nonlinear Dynamic Analysis

In this section, we obtain partial differential equations of dynamic equilibrium of a linear and nonlinear nanobeam, which governs the transverse displacement $z(x,t)$, by substituting $w(x,t)$ from Eq. (16) into Eq. (13). After

Table 2: Comparison of pull-in voltages obtained from the proposed model as mentioned in Eq. (20) with that proposed by [46], [47] and [41], respectively.

Dimensions and Material Properties	Pull-in voltage (V)			
	Chao *et al* [46]	Fang and Pu [47]	Pandey [41]	Eq. (20) with $\mu = 0$, $\tau^0 = 0, E^s = 0$
$b = 150\,\text{nm}$, h = $100\,\text{nm}$, L = $15\,\mu\text{m}$, $d = 300\,\text{nm}$, $E = 226\,\text{GPa}$, $\rho = 3158\,\frac{kg}{m^3}$, $N_0 = 1.35\,\mu\text{N}$	15.7	15.4	17.1	14.56

expanding the forcing term about $z = 0$ and using the static equation given by Eq. (17), the simplified form of the dynamic equation is given by

$$
\begin{aligned}
z_{tt} - \mu z_{xxtt} + z_{xxxx} = \beta_1[z_x^2 + 2z_{sx}z_x]z_{sxx} - \beta_2[z_x^2 + 2z_{sx}z_x]z_{sxxxx} \\
+[\alpha_1 + \beta_1(z_{sx}^2 + z_x^2 + 2z_{sx}z_x)]z_{xx} - [\alpha_2 + \beta_2(z_{sx}^2 + z_x^2 + 2z_{sx}z_x)]z_{xxxx} \\
-\beta_3\Big[z_{xx}^2 + 2z_{sxx}z_{xx} + z_x z_{sxxx} + z_{sx}z_{xxx} + z_x z_{xxx}\Big]z_{sxx} - \beta_3\Big[z_{sxx}^2 + z_{xx}^2 \\
+2z_{sxx}z_{xx} + z_{sx}z_{sxxx} + z_x z_{sxxx} + z_{sx}z_{xxx} + z_x z_{xxx}\Big]z_{xx} - k_1 z_t \\
+k_2 z_{xxt} + \frac{2f_{11}zV_{dc}^2}{(1-z_s)^3}z + \frac{f_{11}(2V_{dc}v(t) + v(t)^2)}{(1-z_s)^2}\left[1 + \frac{2}{(1-z_s)}z\right] - \frac{f_{12}z_{xx}{V_{dc}}^2}{(1-z_s)^3} \\
-3\,\frac{f_{12}\left(z_{sxx} + z_{xx}\right)z{V_{dc}}^2}{\left(1-z_s\right)^4} - \frac{f_{12}\left(z_{sxx} + z_{xx}\right)\left(2\,V_{dc}v\left(t\right) + \left(v\left(t\right)\right)^2\right)}{\left(1-z\right)^3} \\
\left[1 + \frac{3}{(1-z_s)}z\right] - \frac{f_{13}\left({z_x}^2 + 2\,z_{sx}z_x\right)V_{dc}^2}{\left(1-z_s\right)^4} - 4\,\frac{f_{13}\left({z_{sx}}^2 + {z_x}^2 + 2\,z_{sx}z_x\right)z{V_{dc}}^2}{\left(1-z_s\right)^5} \\
-\frac{f_{13}\left({z_{sx}}^2 + {z_x}^2 + 2\,z_{sx}z_x\right)\left(2\,V_{dc}v\left(t\right) + \left(v\left(t\right)\right)^2\right)}{\left(1-z_s\right)^4}\left[1 + \frac{4}{(1-z_s)}z\right] \\
+\frac{f_{21}z{V_{dc}}^2}{\left(1-z_s\right)^2} + \frac{f_{21}(2V_{dc}v(t) + v(t)^2)}{(1-z_s)}\left[1 + \frac{1}{(1-z_s)}z\right] - \frac{f_{22}z_{xx}{V_{dc}}^2}{\left(1-z_s\right)^2}
\end{aligned}
$$

Table 3: Comparison of pull-in voltage obtained from Eq. (20) with that obtained by Nayfeh *et al* [40]

Dimensions and Material Properties	Pull-in voltage (V)	
	Nayfeh *et al* [40]	Eq.(19) with $\mu = 0, \tau^0 = 0, E^s = 0$
$b = 100\,\mu$m, $h = 1.5\ \mu$ m, $L = 510\,\mu$m, $d = 1.18\,\mu$m, $E = 166\,$GPa, $\rho = 2330\,\frac{\text{kg}}{\text{m}^3}$, $N_0 = 170\ \mu$N	4.8	4.4

$$
\begin{aligned}
&-2\,\frac{f_{22}\left(z_{sxx}+z_{xx}\right)z{V_{dc}}^2}{\left(1-z_s\right)^3}-\frac{f_{22}\left(z_{sxx}+z_{xx}\right)\left(2\,V_{dc}v\left(t\right)+\left(v\left(t\right)\right)^2\right)}{\left(1-z_s\right)^2}\\
&\left[1+\frac{2}{\left(1-z_s\right)}z\right]-\frac{f_{23}\left({z_x}^2+2\,z_{sx}z_x\right){V_{dc}}^2}{\left(1-z_s\right)^3}-3\,\frac{f_{23}\left({z_{sx}}^2+{z_x}^2+2\,z_{sx}z_x\right)z{V_{dc}}^2}{\left(1-z_s\right)^4}\\
&-\frac{f_{23}\left({z_{sx}}^2+{z_x}^2+2\,z_{sx}z_x\right)\left(2\,V_{dc}v\left(t\right)+\left(v\left(t\right)\right)^2\right)}{\left(1-z_s\right)^3}\left[1+\frac{3}{\left(1-z_s\right)}z\right]
\end{aligned}
\tag{21}
$$

4.1. Linear modal dynamic equation

To find the partial differential equations of dynamic equilibrium of a linear nanobeam, we neglect the nonlinear terms and dynamic forcing terms in Eq. (21), and get the following form of the equation

$$
\begin{aligned}
z_{tt}-\mu z_{xxtt}+z_{xxxx}&=\beta_1[2z_{sx}z_x]z_{sxx}-\beta_2[2z_{sx}z_x]z_{sxxxx}+[\alpha_1+\beta_1(z_{sx}^2)]\\
&z_{xx}-[\alpha_2+\beta_2(z_{sx}^2)]z_{xxxx}-\beta_3\Big[2z_{sxx}z_{xx}+z_xz_{sxxx}+z_{sx}z_{xxx}\Big]z_{sxx}\\
&-\beta_3\Big[z_{sxx}^2+z_{sx}z_{sxxx}\Big]z_{xx}+\frac{2f_{11}V_{dc}^2}{(1-z_s)^3}z-\frac{f_{12}V_{dc}^2z_{xx}}{(1-z_s)^3}-3\frac{f_{12}V_{dc}^2z_{sxx}}{(1-z_s)^4}z\\
&-2\frac{f_{13}V_{dc}^2z_{sx}z_x}{(1-z_s)^4}-4\frac{f_{13}V_{dc}^2{z_{sx}}^2}{(1-z_s)^5}z+\frac{f_{21}V_{dc}^2}{(1-z_s)^2}z-\frac{f_{22}z_{xx}V_{dc}^2}{(1-z_s)^2}\\
&-2\frac{f_{22}z_{sxx}V_{dc}^2}{(1-z_s)^3}z-2\frac{f_{23}z_{sx}z_xV_{dc}^2}{(1-z_s)^3}-3\frac{f_{23}z_{sx}^2V_{dc}^2}{(1-z_s)^4}z.
\end{aligned}
\tag{22}
$$

To convert the above equation into standard modal dynamic equation, we assume the static and dynamic solutions based on the single mode approximation

as $z(x,t) = P(t)\phi(x)$ and $z_s(x) = q\phi(x)$, respectively, where $\phi(x)$ is exact mode shape given by Eq. (18). Substituting $z(x,t)$ and $z_s(x)$ into above Eq. (22) and then applying Galerkin method, the equation reduces to linear modal dynamic equation as follow:

$$MP_{tt}(t) + KP(t) = 0, \quad \omega = \sqrt{\frac{K}{M}} \tag{23}$$

where,

$M = -10\,q^3 J_{38} + 5\,qJ_6\mu - 5\,q^4 J_{25}\mu + 10\,q^3 J_{22}\mu + J_2 + q^5 J_{32}\mu - 10\,q^2 J_{11}\mu$
$- \mu\,J_5 + 5\,q^4 J_{39} + 10\,q^2 J_{17} - 5\,qJ_8 - q^5 J_{40},$
$K = 2\,J_{10} f_{13} q {V_{dc}}^2 - f_{22} q^2 J_{11} {V_{dc}}^2 + 2\,J_{10} f_{23} q {V_{dc}}^2 + 2\,f_{13} q^2 J_{16} {V_{dc}}^2 - 2\,f_{12} q^2$
$J_{11} {V_{dc}}^2 + f_{21} {V_{dc}}^2 J_{38} q^3 + 4\,f_{11} {V_{dc}}^2 J_8 q - 2\,f_{11} {V_{dc}}^2 J_{17} q^2 + 3\,f_{21} {V_{dc}}^2 J_8 q$
$+ q^5 J_{32}\alpha_1 + 10\,q^3 J_{22}\alpha_1 - 5\,qJ_9\alpha_2 + J_5 f_{12} {V_{dc}}^2 - 10\,q^2 J_{11}\alpha_1 - 10\,q^3 J_{18}\alpha_2$
$+ J_5 f_{22} {V_{dc}}^2 + J_4 - 5\,qJ_9 - 10\,q^3 J_{18} + 10\,q^2 J_{12} + 5\,qJ_6\alpha_1 + 10\,q^2 J_{12}\alpha_2$
$+ 5\,q^4 J_{23}\alpha_2 - f_{21} {V_{dc}}^2 J_2 - 3\,q^7 J_{36}\beta_2 - 3\,f_{21} {V_{dc}}^2 J_{17} q^2 + 5\,q^4 J_{23} + J_4\alpha_2$
$- J_5\alpha_1 + 15\,q^3 J_{20}\beta_1 - 2\,f_{11} {V_{dc}}^2 J_2 - 15\,q^3 J_{19}\beta_2 - 30\,q^4 J_{27}\beta_1 + 30\,q^5 J_{29}\beta_1$
$+ 15\,q^6 J_{31}\beta_2 - 15\,q^6 J_{30}\beta_1 - 30\,q^5 J_{28}\beta_2 + 3\,q^7 J_{35}\beta_1 - f_{23} q^3 J_{37} {V_{dc}}^2$
$+ f_{12} q J_6 {V_{dc}}^2 + f_{22} q^3 J_{22} {V_{dc}}^2 - f_{22} q J_6 {V_{dc}}^2 - 5\,q^4 J_{25}\alpha_1 - q^5 J_{33}\alpha_2$
$- 3\,J_{13}\beta_1 q^2 + 3\,J_{15}\beta_2 q^2 + 30\,q^4 J_{26}\beta_2 - q^5 J_{33} - f_{23} q^2 J_{16} {V_{dc}}^2$
$+ 3\,\beta_3 q^2 J_{41} + 3\,\beta_3 q^2 J_{42} - 15\,\beta_3 q^3 J_{43} - 15\,\beta_3 q^3 J_{44} + 30\,\beta_3 q^4 J_{45}$
$+ 30\,\beta_3 q^4 J_{46} - 30\,\beta_3 q^5 J_{47} - 30\,\beta_3 q^5 J_{48} + 15\,\beta_3 q^6 J_{49}$
$+ 15\,\beta_3 q^6 J_{50} - 3\,\beta_3 q^7 J_{51} - 3\,\beta_3 q^7 J_{52}.$

where, all J's are mentioned in appendix A. The linear frequency obtained from Eq. (23) can be used to find resonance frequency at different bias voltages $V_{\rm dc}$ under the influence of surface and nonlocal effects. The discussion on surface and nonlocal effects on frequency variation will be presented later in the subsequent sections.

4.2. Nonlinear modal dynamic equation

In this section, we obtain nonlinear modal dynamic equation governing the transverse displacement $z(x,t)$ about an equilibrium position given by static

deflection $z_s(x)$. Subsequently, we derive approximate solution based on the method of multiple scale (MMS) to capture the surface and nonlocal effects.

To find the modal dynamic equation, we again assume the dynamic and static solution based on single mode approximation $z(x,t) = P(t)\phi(x)$ and $z_s(x) = q\phi(x)$, respectively. After substituting $z(x,t)$ and $z_s(x)$ into Eq. (21) and using Galerkin method, the equation reduces to nonlinear modal dynamic equation as

$$\begin{aligned} s_{11}P_{tt}(t) + s_{12}P(t) + s_{13}P_t(t) + s_{14}P(t)^2 + s_{15}P(t)^3 + s_{21}V_{dc}V_{ac}\cos(\Omega t) \\ +s_{22}V_{ac}^2\cos^2(\Omega t) + s_{23}V_{dc}V_{ac}\cos(\Omega t)P(t) + s_{24}V_{ac}^2\cos^2(\Omega t)P(t) + s_{25}V_{dc}^2P(t)^2 \\ s_{26}V_{dc}V_{ac}\cos(\Omega t)P(t)^2 + s_{27}V_{ac}^2\cos^2(\Omega t)P(t)^2 + s_{28}V_{dc}^2P(t)^3 \\ +s_{29}V_{dc}V_{ac}\cos(\Omega t)P(t)^3 + s_{30}V_{ac}^2\cos^2(\Omega t)P(t)^3 = 0 \end{aligned} \tag{24}$$

where,

$s_{11} = M,\ s_{12} = K,$

$s_{13} = k_1J_2 + q^5k_2J_{32} - 10\,q^2k_2J_{11} + 10\,q^3k_2J_{22} - 5\,q^4k_2J_{25} + 5\,qk_2J_6 - k_2J_5$
$- 5\,qJ_8k_1 + 10\,q^2J_{17}k_1 - 10\,q^3J_{38}k_1 + 5\,q^4J_{39}k_1 - q^5J_{40}k_1,$

$s_{14} = -15\,q^2\beta_2J_{19} + 30\,q^3\beta_2J_{26} - 15\,q^5\beta_1J_{30} - 30\,q^4\beta_2J_{28} - 3\,\beta_1qJ_{13} + 3\,q^6\beta_1J_{35}$
$+ 15\,q^2\beta_1J_{20} + 15\,q^5\beta_2J_{31} + 3\,\beta_2qJ_{15} - 30\,q^3\beta_1J_{27} - 3\,q^6\beta_2J_{36} + 30\,q^4\beta_1J_{29}$
$+ 3\,\beta_3qJ_{41} + 3\,\beta_3qJ_{42} + 15\,\beta_3q^5J_{49} - 15\,\beta_3q^2J_{43} - 15\,\beta_3q^2J_{44} - 3\,\beta_3q^6J_{51}$
$+ 30\,\beta_3q^3J_{45} + 30\,\beta_3q^3J_{46} - 30\,\beta_3q^4J_{47} - 30\,\beta_3q^4J_{48} + 15\,\beta_3q^5J_{50} - 3\,\beta_3q^6J_{52},$

$s_{15} = 5\,q^4\beta_2J_{31} + \beta_2J_{15} - 10\,q^3\beta_2J_{28} + q^5\beta_1J_{35} - 5\,q^4\beta_1J_{30} - \beta_1J_{13} - 5\,q\beta_2J_{19}$
$+ 5\,q\beta_1J_{20} - q^5\beta_2J_{36} - 10\,q^2\beta_1J_{27} + 10\,q^2\beta_2J_{26} + 10\,q^3\beta_1J_{29} + \beta_3J_{41}$
$- 5\,\beta_3qJ_{43} + 10\,\beta_3q^2J_{45} + 10\,\beta_3q^2J_{46} - 10\,\beta_3q^3J_{47} - 10\,\beta_3q^3J_{48} + \beta_3J_{42}$
$+ 5\,\beta_3q^4J_{49} + 5\,\beta_3q^4J_{50} - 5\,\beta_3qJ_{44} - \beta_3q^5J_{51} - \beta_3q^5J_{52},$

$s_{21} = -6\,f_{11}q^2J_8 - 4\,f_{12}q^2J_6 + 2\,f_{12}q^3J_{11} + 2\,f_{11}q^3J_{17} + 8\,f_{21}q^3J_{17} - 2\,f_{21}q^4J_{38}$
$- 2\,J_1f_{11} - 2\,J_1f_{21} - 6\,f_{22}q^2J_6 + 6\,f_{22}q^3J_{11} - 2\,f_{22}q^4J_{22} + 6\,f_{11}qJ_2$
$+ 2\,f_{22}qJ_5 + 2\,f_{12}qJ_5 - 2\,f_{13}q^3J_{16} + 2\,f_{23}q^4J_{37} - 4\,f_{23}q^3J_{16}$
$+ 2\,f_{13}q^2J_{10} + 2\,J_{10}f_{23}q^2 - 12\,f_{21}q^2J_8 + 8\,f_{21}qJ_2,$

$s_{22} = -2\,f_{12}q^2J_6 - J_1f_{11} - J_1f_{21} + 4\,f_{21}qJ_2 + 3\,f_{11}qJ_2 - 3\,f_{11}q^2J_8 + f_{12}q^3J_{11}$

$$
\begin{aligned}
&+ f_{13}q^2J_{10} + f_{11}q^3J_{17} + f_{23}q^2J_{10} - f_{13}q^3J_{16} + f_{23}q^4J_{37} + f_{12}qJ_5\\
&+ f_{22}qJ_5 - f_{22}q^4J_{22} - 6\,f_{21}q^2J_8 + 4\,f_{21}q^3J_{17} - f_{21}q^4J_{38}\\
&- 2\,f_{23}q^3J_{16} - 3\,f_{22}q^2J_6 + 3\,f_{22}q^3J_{11},\\
s_{23} &= 4\,f_{13}q^2J_{16} + 2\,f_{21}J_{38}q^3 + 4\,f_{13}qJ_{10} - 4\,f_{11}J_{17}q^2 + 6\,f_{21}J_8q - 6\,f_{21}J_{17}q^2\\
&- 2\,f_{21}J_2 - 2\,f_{22}qJ_6 - 2\,f_{22}q^2J_{11} + 2\,f_{22}q^3J_{22} + 2\,f_{12}qJ_6 - 4\,f_{12}q^2J_{11}\\
&+ 4\,f_{23}qJ_{10} - 2\,f_{23}q^2J_{16} - 2\,f_{23}q^3J_8 + 8\,f_{11}J_{37}q\\
&+ 2\,J_5f_{22} + 2\,J_5f_{12} - 4\,f_{11}J_2,\\
s_{24} &= J_5f_{12} + J_5f_{22} - 2\,f_{11}J_2 - f_{21}J_2 + 2\,f_{23}qJ_{10} - 2\,f_{12}q^2J_{11} + f_{12}qJ_{16} +\\
&f_{22}q^3J_{22} + f_{21}J_{38}q^3 - 2\,f_{11}J_{17}q^2 + 3\,f_{21}J_8q - 3\,f_{21}J_{17}q^2 + 2\,f_{13}qJ_{10}\\
&+ 2\,f_{13}q^2J_{16} - f_{23}q^3J_{37} - f_{23}q^2J_{16} - f_{22}q^2J_{11} + 4\,f_{11}J_8q - f_{22}qJ_6,\\
s_{25} &= 3\,f_{12}J_6 + 2\,f_{22}J_{22}q^2 + f_{13}J_{10} + f_{23}J_{10} - 4\,f_{22}J_{11}q + 2\,f_{22}J_6 + 7\,f_{13}qJ_{16}\\
&+ 4\,f_{23}qJ_{16} - 5\,f_{23}q^2J_{37} - 3\,f_{12}J_{11}q,\\
s_{26} &= 4\,f_{22}J_6 - 10\,f_{23}q^2J_{37} + 4\,f_{22}J_{22}q^2 + 6\,f_{12}J_6 - 6\,f_{12}J_{11}q - 8\,f_{22}J_{11}q\\
&+ 2\,f_{23}J_{10} + 8\,f_{23}qJ_{16} + 2\,f_{13}J_{10} + 14\,f_{13}qJ_{16},\\
s_{27} &= 3\,f_{12}J_6 + 2\,f_{22}J_{22}q^2 + f_{13}J_{10} + f_{23}J_{10} - 4\,f_{22}J_{11}q + 2\,f_{22}J_6 + 7\,f_{13}qJ_{16}\\
&+ 4\,f_{23}qJ_{16} - 5\,f_{23}q^2J_{37} - 3\,f_{12}J_{11}q,\\
s_{28} &= 3\,f_{23}J_{16} - 3\,f_{23}J_{37}q + 4\,f_{13}J_{16}, \quad s_{29} = -6\,f_{23}J_{37}q + 6\,f_{23}J_{16} + 8\,f_{13}J_{16},\\
s_{30} &= 3\,f_{23}J_{16} - 3\,f_{23}J_{37}q + 4\,f_{13}J_{16}.
\end{aligned}
$$

Here, all J's are given in appendix A. After dividing Eq. (24) by s_{11}, the simplified form of equation is given by

$$
\begin{aligned}
&P_{tt}(t) + b_1P(t) + b_2P_t(t) + b_3P(t)^2 + b_4P(t)^3 + b_5V_{dc}V_{ac}\cos(\Omega t)\\
&+b_6V_{ac}^2\cos^2(\Omega t) + b_7V_{dc}V_{ac}\cos(\Omega t)P(t) + b_8V_{ac}^2\cos^2(\Omega t)P(t) + b_9V_{dc}^2P(t)^2\\
&b_{10}V_{dc}V_{ac}\cos(\Omega t)P(t)^2 + b_{11}V_{ac}^2\cos^2(\Omega t)P(t)^2 + b_{12}V_{dc}^2P(t)^3\\
&+b_{13}V_{dc}V_{ac}\cos(\Omega t)P(t)^3 + b_{14}V_{ac}^2\cos^2(\Omega t)P(t)^3 = 0 \qquad (25)
\end{aligned}
$$

where,

$$
\begin{aligned}
b_1 &= \frac{s_{12}}{s_{11}}, \quad b_2 = \frac{s_{13}}{s_{11}}, \quad b_3 = \frac{s_{14}}{s_{11}}, \quad b_4 = \frac{s_{15}}{s_{11}}, \quad b_5 = \frac{s_{21}}{s_{11}},\\
b_6 &= \frac{s_{22}}{s_{11}}, \quad b_7 = \frac{s_{23}}{s_{11}}, \quad b_8 = \frac{s_{24}}{s_{11}}, \quad b_9 = \frac{s_{25}}{s_{11}}, \quad b_{10} = \frac{s_{26}}{s_{11}},
\end{aligned}
$$

$$b_{11} = \frac{s_{27}}{s_{11}}, \quad b_{12} = \frac{s_{28}}{s_{11}}, \quad b_{13} = \frac{s_{29}}{s_{11}}, \quad b_{14} = \frac{s_{30}}{s_{11}}$$

4.3. Method of multiple scales

In this section, we apply method of multiple scales to obtain the modulation equations. In order to apply the method of multiple scales, we convert the damping term, nonlinear stiffness terms and forcing terms in Eq. (25) into weak terms by re-scaling them with ϵ, respectively, as follow

$$\begin{aligned} P_{tt}(t) + b_1 P(t) + \epsilon b_2 P_t(t) + \epsilon b_3 P(t)^2 + \epsilon b_4 P(t)^3 + \epsilon b_5 V_{dc} V_{ac} \cos(\Omega t) \\ + \epsilon b_6 V_{ac}^2 \cos^2(\Omega t) + \epsilon b_7 V_{dc} V_{ac} \cos(\Omega t) P(t) + \epsilon b_8 V_{ac}^2 \cos^2(\Omega t) P(t) \\ + \epsilon b_9 V_{dc}^2 P(t)^2 + \epsilon b_{10} V_{dc} V_{ac} \cos(\Omega t) P(t)^2 + \epsilon b_{11} V_{ac}^2 \cos^2(\Omega t) P(t)^2 \\ + \epsilon b_{12} V_{dc}^2 P(t)^3 + \epsilon b_{13} V_{dc} V_{ac} \cos(\Omega t) P(t)^3 + \epsilon b_{14} V_{ac}^2 \cos^2(\Omega t) P(t)^3 = 0. \end{aligned} \quad (26)$$

Assuming the solution of the form $P(t) = \sum_{j=0}^{1} \epsilon^j p_j(T_0, T_1) + \bigcirc(\epsilon^2)$, where, $T_0 = t$ is fast time scale and $T_1 = \epsilon t$ is slow time scale. After substituting the solution in Eq. (26) and comparing the coefficients of different powers of ϵ, we get

$$\bigcirc(\epsilon^0) : D_0^2 p_0 + \omega^2 p_0 = 0, \quad (27)$$

$$\begin{aligned} \bigcirc(\epsilon^1) : D_0^2 p_1 + \omega^2 p_1 = -b_8 {V_{ac}}^2 \left(\cos(\Omega t)\right)^2 p_0 - b_{11} {V_{ac}}^2 \left(\cos(\Omega t)\right)^2 {p_0}^2 \\ - b_{14} {V_{ac}}^2 \left(\cos(\Omega t)\right)^2 {p_0}^3 - b_7 V_{dc} V_{ac} \cos(\Omega t) p_0 - b_{10} V_{dc} V_{ac} \cos(\Omega t) {p_0}^2 \\ - b_{13} V_{dc} V_{ac} \cos(\Omega t) {p_0}^3 - b_3 {p_0}^2 - b_4 {p_0}^3 - b_6 {V_{ac}}^2 \left(\cos(\Omega t)\right)^2 - 2 D_0 D_1 p_0 \\ - b_2 D_0 p_0 - b_9 {V_{dc}}^2 {p_0}^2 - b_{12} {V_{dc}}^2 {p_0}^3 - b_5 V_{dc} V_{ac} \cos(\Omega t), \end{aligned} \quad (28)$$

where, $\omega^2 = b_1$, and the derivatives D_m for $m = 0, ..., 1$ are defined as $D_m = \frac{\partial}{\partial T_m} \frac{dT_m}{dt}$. Assuming the solution of Eq. (27) as

$$p_0 = A(T_1) e^{(i\omega T_0)} + \bar{A}(T_1) e^{(-i\omega T_0)} \quad (29)$$

where, $A(T_1)$ and $\bar{A}(T_1)$ are complex conjugates of each other, and substituting it into Eq. (28) with detuning parameter σ as defined in $\Omega = \omega + \epsilon\sigma$, we get

$$D_0^2 p_1 + \omega^2 p_1 = \Bigg[- i\omega 2 D_1 A - i\omega b_2 A - 3 b_4 A^2 \bar{A} - b_5 \frac{V_{dc} V_{ac}}{2} e^{(i\sigma T_1)}$$

$$-b_8\left(\frac{{V_{ac}}^2}{2}A+\frac{{V_{ac}}^2}{4}\bar{A}e^{(2i\sigma T_1)}\right)-b_{10}\frac{V_{dc}V_{ac}}{2}\left(A^2e^{(-i\sigma T_1)}+2A\bar{A}e^{(i\sigma T_1)}\right)$$
$$-3b_{12}A^2\bar{A}{V_{dc}}^2-b_{14}\left(\frac{{V_{ac}}^2}{2}3A^2\bar{A}+\frac{{V_{ac}}^2}{4}\left(A^3e^{(-2i\sigma T_1)}+3A\bar{A}^2e^{(2i\sigma T_1)}\right)\right)\Bigg]e^{(i\omega T_0)}$$
$$+\Bigg[-b_3A^2-b_6\frac{{V_{ac}}^2}{4}e^{(2i\sigma T_1)}-b_7\frac{V_{dc}V_{ac}}{2}Ae^{(i\sigma T_1)}-b_9{V_{dc}}^2A^2$$
$$-b_{11}\left(\frac{{V_{ac}}^2}{2}A^2+\frac{{V_{ac}}^2}{4}2A\bar{A}e^{(2i\sigma T_1)}\right)-b_{13}\frac{V_{dc}V_{ac}}{2}\left(A^3e^{(-i\sigma T_1)}+3A^2\bar{A}e^{(i\sigma T_1)}\right)\Bigg]$$
$$e^{(2i\omega T_0)}+\Bigg[-b_4A^3-b_8\frac{{V_{ac}}^2}{4}Ae^{(2i\sigma T_1)}-b_{10}\frac{V_{dc}V_{ac}}{2}A^2e^{(i\sigma T_1)}-b_{12}{V_{dc}}^2A^3$$
$$-b_{14}\left(\frac{{V_{ac}}^2}{2}A^3+\frac{{V_{ac}}^2}{4}3A^2\bar{A}e^{(2i\sigma T_1)}\right)\Bigg]e^{(3i\omega T_0)}+\Bigg[-b_{11}\frac{{V_{ac}}^2}{4}A^2e^{(2i\sigma T_1)}$$
$$-b_{13}\frac{V_{dc}V_{ac}}{2}A^3e^{(i\sigma T_1)}\Bigg]e^{(4i\omega T_0)}-\left[b_{14}\frac{{V_{ac}}^2}{4}A^3e^{(2i\sigma T_1)}\right]e^{(5i\omega T_0)}-2b_3A\bar{A}-b_6\frac{{V_{ac}}^2}{2}$$
$$-b_7\frac{V_{dc}V_{ac}}{2}Ae^{(-i\sigma T_1)}-2b_9{V_{dc}}^2A\bar{A}-b_{11}\left({V_{ac}}^2A\bar{A}+\frac{{V_{ac}}^2}{4}A^2e^{(-2i\sigma T_1)}\right)$$
$$-3b_{13}\frac{V_{dc}V_{ac}}{2}A\bar{A}^2e^{(i\sigma T_1)}+cc \tag{30}$$

where, cc represents complex conjugate terms. After eliminating secular terms from Eq. (30), we get the following complex modulation equation

$$-i\omega 2D_1A-i\omega b_2A-3b_4A^2\bar{A}-b_5\frac{V_{dc}V_{ac}}{2}e^{(i\sigma T_1)}-b_8\left(\frac{{V_{ac}}^2}{2}A+\frac{{V_{ac}}^2}{4}\right.$$
$$\left.\bar{A}e^{(2i\sigma T_1)}\right)-b_{10}\frac{V_{dc}V_{ac}}{2}\left(A^2e^{(-i\sigma T_1)}+2A\bar{A}e^{(i\sigma T_1)}\right)-3b_{12}A^2\bar{A}{V_{dc}}^2$$
$$-b_{14}\left(\frac{{V_{ac}}^2}{2}3A^2\bar{A}+\frac{{V_{ac}}^2}{4}\left(A^3e^{(-2i\sigma T_1)}+3A\bar{A}^2e^{(2i\sigma T_1)}\right)\right)=0. \tag{31}$$

To convert the above equation into real modulation equation, we assume the polar form of $A=\frac{ae^{(i\theta)}}{2}$, $\bar{A}=\frac{\bar{a}e^{-i\theta}}{2}$ and substitute it into Eq. (31). After separating and equating the real and imaginary terms, we obtain following form of modulation equation

$$a'=-t_1a-t_2\sin(\phi)-t_3a\sin(2\phi)-t_4a^2\sin(\phi)-t_5a^3\sin(2\phi), \tag{32}$$
$$a\phi'=a\sigma-t_6a^3-t_2\cos(\phi)-t_7a-t_3a\cos(2\phi)-t_8a^2\cos(\phi)$$

$$-t_9 a^3 \cos(2\phi). \qquad (33)$$

where,

$$t_1 = \frac{b_2}{2}, \quad t_2 = \frac{b_5 V_{dc} V_{ac}}{2\omega}, \quad t_3 = \frac{b_8 {V_{ac}}^2}{8\omega}, \quad t_4 = \frac{b_{10} V_{dc} V_{ac}}{8\omega},$$
$$t_5 = \frac{b_{14} {V_{ac}}^2}{16\omega}, \quad t_6 = \left(\frac{3b_4}{8\omega} + \frac{3b_{12} {V_{dc}}^2}{8\omega} + \frac{3b_{14} {V_{ac}}^2}{16\omega} \right), \; t_7 = 2t_3,$$
$$t_8 = 3t_4, \quad t_9 = 2t_5, \quad a' = \frac{da}{dT_1}, \quad \phi' = \frac{d\phi}{dT_1}, \quad \phi = \sigma T_1 - \theta.$$

The non-trivial equilibrium solutions of Eqs. (32) and (33) can be obtained by solving $a' = 0$ and $\phi' = 0$, simultaneously. In the subsequent section, we do stability analysis of the equilibrium solutions.

4.4. Stability

The stability of equilibrium solutions can be obtained by finding the Jacobian and eigen values of the equilibrium solutions. For Eqs. (32) and (33), the equilibrium solutions are given by

$$-t_1 a - t_2 \sin(\phi) - t_3 a \sin(2\phi) - t_4 a^2 \sin(\phi) - t_5 a^3 \sin(2\phi) = 0, \qquad (34)$$
$$\sigma - t_6 a^2 - \frac{t_2 \cos(\phi)}{a} - t_7 - t_3 \cos(2\phi) - t_8 a \cos(\phi) - t_9 a^2 \cos(2\phi) = 0. \qquad (35)$$

and the corresponding Jacobian matrix and eigen values are given as

$$J = \begin{bmatrix} a_{11} & a_{12} \\ a_{13} & a_{14} \end{bmatrix},$$

where,

$$a_{11} = -t_1 - t_3 \sin(2\phi) - 2\, t_4 a \sin(\phi) - 3\, t_5 a^2 \sin(2\phi),$$
$$a_{12} = -t_2 \cos(\phi) - 2\, t_3 a \cos(2\phi) - t_4 a^2 \cos(\phi) - 2\, t_5 a^3 \cos(2\phi),$$
$$a_{13} = -2\, t_6 a + \frac{t_2 \cos(\phi)}{a^2} - t_8 \cos(\phi) - 2\, t_9 a \cos(2\phi),$$
$$a_{14} = \frac{t_2 \sin(\phi)}{a} + 2\, t_3 \sin(2\phi) + t_8 a \sin(\phi) + 2\, t_9 a^2 \sin(2\phi).$$

and

$$\lambda_{1,2} = -\frac{1}{2a}\left(\lambda_A \pm \sqrt{\lambda_B} \right)$$

where,

$$\lambda_A = -4\,a^3 t_9 \sin(\phi)\cos(\phi) + 6\,a^3 t_5 \sin(\phi)\cos(\phi) - t_8 a^2 \sin(\phi) + 2\,t_4 a^2 \sin(\phi)$$
$$-2\,a t_3 \sin(\phi)\cos(\phi) + t_1 a - t_2 \sin(\phi),$$
$$\lambda_B = -24\,(\cos(\phi))^3 a^5 t_5 t_4 - 8\,(\cos(\phi))^3 a^5 t_9 t_8 + 32\,(\cos(\phi))^2 t_6 a^4 t_3 + {t_1}^2 a^2$$
$$+{t_8}^2 a^4 - 5\,{t_2}^2 (\cos(\phi))^2 + 4\,{t_4}^2 a^4 + 8\,t_6 a^3 t_2 \cos(\phi) + 8\,t_6 a^5 t_4 \cos(\phi)$$
$$-8\,t_2 (\cos(\phi))^2 t_4 a^2 + 2\,t_8 (\cos(\phi))^2 a^2 t_2 + 2\,a t_2 \sin(\phi)\,t_1 + 2\,t_8 a^3 \sin(\phi)\,t_1$$
$$+20\,t_2 \cos(\phi)\,t_3 a + 20\,t_2 \cos(\phi)\,t_5 a^3 + 4\,t_8 \cos(\phi)\,a^5 t_5 + 8\,t_9 a^5 t_4 \cos(\phi)$$
$$+24\,t_3 \cos(\phi)\,a^3 t_4 + 4\,t_8 (\cos(\phi))^3 a^3 t_3 - 24\,t_3 (\cos(\phi))^3 a^3 t_4 - 28\,t_2 (\cos(\phi))^3$$
$$t_3 a - 28\,t_2 (\cos(\phi))^3 t_5 a^3 + 4\,t_8 (\cos(\phi))^3 a^5 t_5 + 8\,t_9 a^3 t_2 (\cos(\phi))^3 + 4\,t_4 a^3 \sin(\phi)\,t_1$$
$$+4\,t_8 a^3 t_3 \cos(\phi) + 8\,t_9 a^5 \cos(\phi)\,t_8 + 24\,a^5 t_5 \cos(\phi)\,t_4 - 16\,t_9 a^6 (\cos(\phi))^2 t_5$$
$$-16\,t_9 a^4 (\cos(\phi))^2 t_3 + 72\,a^4 t_5 (\cos(\phi))^2 t_3 + 32\,(\cos(\phi))^2 t_6 a^6 t_5 + 16\,(\cos(\phi))^4$$
$$t_9 a^6 t_5 + 16\,(\cos(\phi))^4 t_9 a^4 t_3 - 72\,(\cos(\phi))^4 t_3 a^4 t_5 + 12\,t_3 \sin(\phi)\cos(\phi)\,a^2 t_1$$
$$+8\,t_9 a^4 \sin(\phi)\cos(\phi)\,t_1 + 12\,a^4 t_5 \sin(\phi)\cos(\phi)\,t_1 + 16\,a^6 {t_9}^2 (\cos(\phi))^2 + 36\,a^6 {t_5}^2$$
$$(\cos(\phi))^2 + 36\,a^2 {t_3}^2 (\cos(\phi))^2 - (\cos(\phi))^2 {t_8}^2 a^4 - 4\,(\cos(\phi))^2 {t_4}^2 a^4 - 16$$
$$(\cos(\phi))^4 a^6 {t_9}^2 - 36\,(\cos(\phi))^4 a^6 {t_5}^2 - 36\,(\cos(\phi))^4 {t_3}^2 a^2 - 16\,t_6 a^4 t_3 - 16\,t_6 a^6 t_5$$
$$+16\,t_9 a^4 t_3 + 16\,t_9 a^6 t_5 + 4\,t_2 t_4 a^2 + 4\,t_8 a^4 t_4 + 2\,t_8 a^2 t_2 + {t_2}^2.$$

Finally, the condition under which the equilibrium solutions become stable is given by $\mathrm{Re}(\lambda_{1,2}) < 0$.

5. Results and discussions

In this section, we study the influence of surface and nonlocal effects first on the pull-in voltage and frequency of a linear nanobeam, and then on the frequency response of a nonlinear nanobeam. To do these analysis, we take the dimensions and material properties from [41, 48], and the corresponding surface and nonlocal parameters from [12] as mentioned in Table (4).

Table 4: Dimensions and material properties of a nanobeam

Quantity	Symbol	
Length	L	15 μm
Width	b	150 nm
Height	h	100 nm
Gap	d	300 nm
Young's modulus	E	226×10^9 N/m^2
Pretension	N_0	1.35 μN
Density	ρ	3158 kg/m^3
Electric constant	ϵ_0	8.854×10^{-12} F/m
Residual surface tension	τ^0	0.9108 N/m
Elastic surface modulus	E^s	5.1882 N/m

5.1. Pull-in voltage and frequency of linear system vibrations

In this section, we study the influence of surface and nonlocal effects on pull-in voltage and frequency of linear system vibrations. The pull-in voltage is obtained by first solving Eq. (19) and then substituting the results in Eq. (20). The validation of the approach has also been presented in Tables 2 and 3, respectively, without considering the surface and nonlocal effects. Figure 2(a) shows the variation of pull-in voltage with and without surface effects when the nonlocal is neglected. It is found that for $E^s = 0$, $\tau^0 = 0$, $\frac{e_0 a}{L} = 0$, the value of pull-in voltage is 14.6 V and for $E^s = 5.1882\ \mathrm{Nm}^{-1}$, $\tau^0 = 0.9108\ \mathrm{Nm}^{-1}$, $\frac{\mathrm{e_0 a}}{\mathrm{L}} = 0$, the value of pull-in is 16 V. It shows that with surface effects the pull-in voltage is increased by about 9%. Similarly, the pull-in voltage with or without nonlocal parameter when surface effect is neglected is presented in Fig. 2(b). It shows that the pull-in voltage increases approximately by 59.5% as the nonlocal parameter, $\frac{e_0 a}{L}$, is varied from 0 to 0.8. Finally, we study the combined effect of both surface and nonlocal parameters on pull-in voltage Fig. 2(c). It shows that for fixed surface parameters, i.e., $E^s = 5.1882\ \mathrm{Nm}^{-1}$, $\tau^0 = 0.9108\ \mathrm{Nm}^{-1}$, pull-in voltage increases by around 62% as the nonlocal parameter $\frac{e_0 a}{L}$ varies from 0 to 0.8.

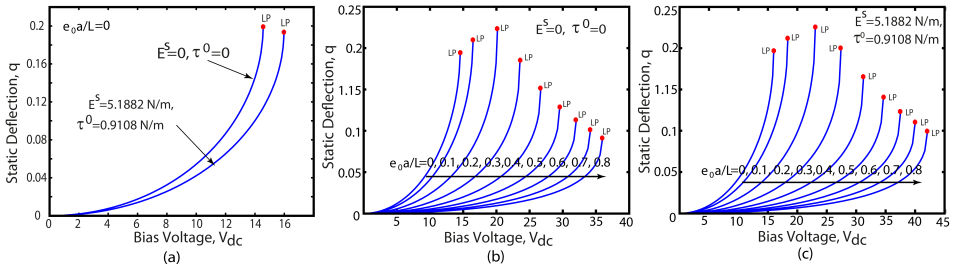

Figure 2: Variation of static deflection with dc bias voltage (a) with or without surface effects, (b) for different values of non-local parameters varying from 0 to 0.8, and (c) for combined surface and nonlocal effects.

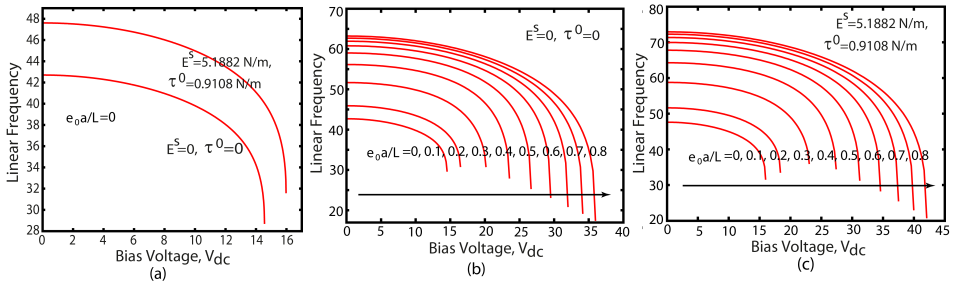

Figure 3: Variation of linear resonance frequency with dc bias voltage (a) with or without surface effects, (b) for different values of non-local parameters varying from 0 to 0.8, and (c) for combined surface and nonlocal effects.

Similarly, the resonance frequency is obtained by first computing the static deflection from Eq. (19) and then substituting it in Eq. (23). To validate procedure for obtaining the resonance frequency, we compute frequency from Eq. (23) under negligible nonlocal and surface effects at $V_{\rm dc} = 0$. Under this condition, we obtain non-dimensional frequency $\omega = 42.7$ and dimensional frequency $f_n = \frac{\omega\omega_s}{2\pi} = 7.37$ MHz, where, $\omega_s = \sqrt{\frac{(EI)_s}{\rho A L^4}}$ is non-dimensional parameter. On comparing $f_n = 7.37$ MHz with 7.6 MHz, as mentioned in [41, 48], we obtain a percentage difference of about 3%. Moreover, the pull-in obtained using frequency variation versus $V_{\rm dc}$ is found to be same as that obtained from the variation of static deflection as shown in Fig. 2(a). Thus, the procedure is validated. Like Fig. 2, Fig. 3 shows the variation of frequency with bias voltage with or without surface and nonlocal effects. Fig-

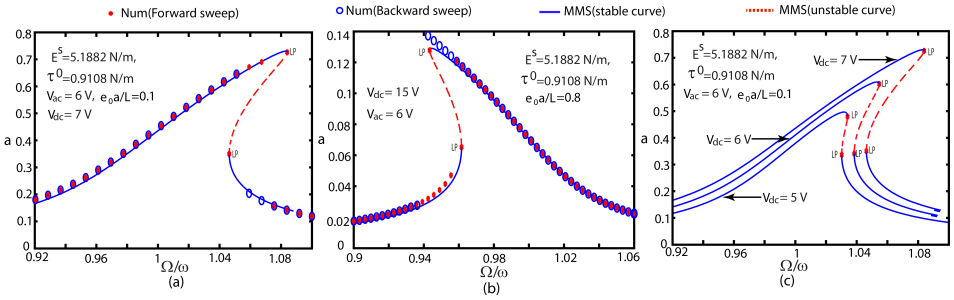

Figure 4: Comparison between solutions obtained from the method of multiple scale and numerical simulation with surface effects captured by $E^s = 5.1882$ N/m, $\tau^0 = 0.9108$N/m for (a) $\frac{e_0 a}{L} = 0.1$, and (b) $\frac{e_0 a}{L} = 0.8$. (c) Variation of frequency of nonlinear system under nonlocal and surface effects denoted by $E^s = 5.1882$ N/m, $\tau^0 = 0.9108$N/m, $\frac{e_0 a}{L} = 0.1$ at different dc bias $\mathrm{V_{dc}} = 5\mathrm{V}, 6\mathrm{V}$ and $7V$ with same $\mathrm{V_{ac}} = 6\mathrm{V}$.

ure 3(a) shows increase in resonance frequency by 10% due to the surface effects, $E^s = 5.1882$ Nm^{-1}, $\tau^0 = 0.9108$ Nm^{-1}. Similarly, the increase in frequency by about 32.5% is found as nonlocal parameter, $\frac{e_0 a}{L}$, increase from 0 to 0.8 as shown in Fig. 3(b). Finally, due to the combined effect of surface ($E^s = 5.1882$ Nm^{-1}, $\tau^0 = 0.9108$ Nm^{-1}) and nonlocal ($\frac{e_0 a}{L} = 0..0.8$), the frequency increases by about 34.7% as shown in Fig. 3(c). Finally, we state that the combined surface and nonlocal effects influence pull-in voltage as well as resonance frequency effectively. The increase in pull-in voltages and linear frequencies in linear regime is due to increase in linear stiffness with the increase in nonlocal and surface effects.

5.2. ***Frequency of nonlinear system vibrations***

In this section, we first validate the nonlinear solution obtained using the methods of multiple scale and then analyse the influence of surface and nonlocal effects. To validate the method of multiple scale, we first solve evolution equations given by Eqs. (32) and (33) using Matlab based Matcont for a given set of parameters. Subsequently, for the same parameter values, we compare the solution of evolution equations with the numerical solution obtained by solving original modal dynamic equation given by Eq. (25) using Runge-Kutta method

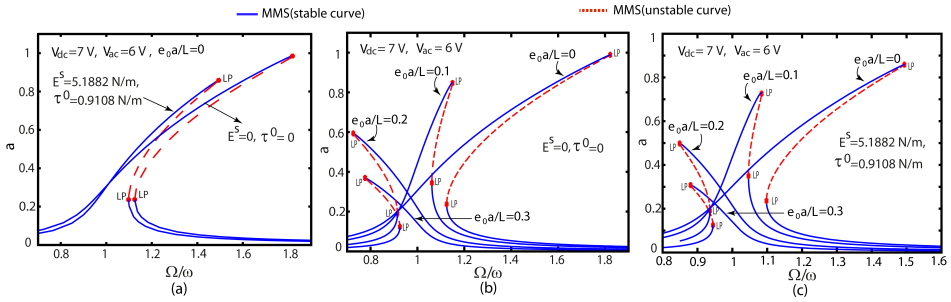

Figure 5: Variation of frequency of nonlinear system for constant electrostatic excitation $V_{\rm dc} = 7V$, $V_{\rm ac} = 6V$ (a) with and without surface effects, (b) with nonlocal effects varying 0 to 0.3, and (c) combined surface and nonlocal effects.

in Fig 4. Figure 4(a) shows that the hardening effect can be captured by the solutions obtained from MMS as well as numerical simulation for the parameter values $E^s = 5.1882$ Nm^{-1}, $\tau^0 = 0.9108$ Nm^{-1}, $\frac{\rm e_0 a}{\rm L} = 0.1$, $\rm V_{dc} = 7$ V, $\rm V_{ac} = 6$V, $\rm Q = 5000$. Similarly, the softening effects can also be captured from the solutions obtained from MMS and numerical simulation, however, for different parameter values given by $E^s = 5.1882$ Nm^{-1}, $\tau^0 = 0.9108$ Nm^{-1}, $\frac{\rm e_0 a}{\rm L} = 0.8, \rm V_{dc} = 15$V, $\rm V_{ac} = 6$V, $\rm Q = 5000$.

After validating the nonlinear response obtained from MMS with numerical solution in Figs. 4(a) and (b), we observe that the nonlinearity increases with increase in the static deflection due to large dc bias as shown in Fig. 4(c) for $E^s = 5.1882$ Nm^{-1}, $\tau^0 = 0.9108$ Nm^{-1}, $\frac{\rm e_0 a}{\rm L} = 0.1$, $\rm V_{ac} = 6$V, $\rm Q = 5000$. For fixed excitation of $V_{\rm dc} = 7V$ and $V_{\rm ac} = 6V$, we also analyse the influence of surface and nonlocal effects in Fig. 5. Figure 5(a) shows frequency of nonlinear system with and without surface effects captured by $E^s = 5.1882$ Nm^{-1}, $\tau^0 = 0.9108$ Nm^{-1} when nonlocal effect is neglected. It is observed that the surface parameter decreases the nonlinear response as the excitation voltage is kept constant. However, it does not effect the nature of nonlinearity. Similarly, we also observe the variation of frequency of nonlinear system with increase in non-local parameters from 0 to 0.3 as shown in Fig. 5(b) in the absence of surface effects. Like surface effects, the nonlinear response also decreases with increase

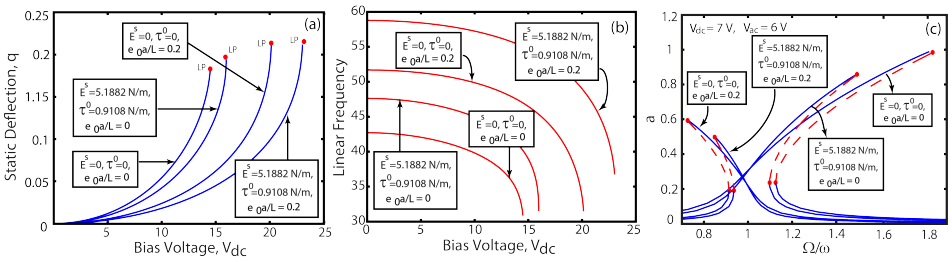

Figure 6: Comparison of variation of (a) static deflection versus $V_{\rm dc}$, (b) linear frequency versus $V_{\rm dc}$ and (c) frequency reponse of nonlinear system under different conditions with case 1 as $E^s = 0,\ \tau^0 = 0,\ \frac{e_0 a}{L} = 0$, case 2 as $E^s = 5.1882\ \text{Nm}^{-1},\ \tau^0 = 0.9108\ \text{Nm}^{-1},\ \frac{\text{e}_0\text{a}}{\text{L}} = 0$, case 3 as $E^s = 0,\ \tau^0 = 0,\ \frac{e_0 a}{L} = 0.2$, and the case 4 with $E^s = 5.1882\ \text{Nm}^{-1},\ \tau^0 = 0.9108\ \text{Nm}^{-1},\ \frac{\text{e}_0\text{a}}{\text{L}} = 0.2$.

in nonlocal effect, but the nature of nonlinearity also changes from hardening to softening when nonlocal parameter increases from 0.1 to 0.3. Such variations in frequency reponse of nonlinear system can also be clearly observed under the combined influence of surface and nonlocal effects in Fig. 5(c). Fig. 6(a) shows the comparison of variation of static deflection versus dc bias voltage for different condition with case 1 as $E^s = 0,\ \tau^0 = 0,\ \frac{e_0 a}{L} = 0$, case 2 as $E^s = 5.1882\ \text{Nm}^{-1},\ \tau^0 = 0.9108\ \text{Nm}^{-1},\ \frac{\text{e}_0\text{a}}{\text{L}} = 0$, case 3 as $E^s = 0,\ \tau^0 = 0,\ \frac{e_0 a}{L} = 0.2$, and the case 4 as $E^s = 5.1882\ \text{Nm}^{-1},\ \tau^0 = 0.9108\ \text{Nm}^{-1},\ \frac{\text{e}_0\text{a}}{\text{L}} = 0.2$,respectively. Similarly, the comparison of variation of linear frequency versus dc bias voltage and frequency response of nonlinear system for different cases are shown in Figs. 6(b) and (c). The comparison shows that nonlocal effect dominates over surface effect for the given surface parameters. However, further studies can be done by improving the surface effect modeling based on Hu *et al* [27, 28] by varying the surface parameters.

Finally, we state that the modeling of surface and nonlocal effects assume significance in computing frequency of linear and nonlinear nanobeams under electrostatic excitation. Similar analysis can also be done to beams of different boundary conditions.

6. Conclusion

In this paper, we have analyzed the influence of nonlocal and surface effects on the static and dynamic response of a fixed-fixed nanobeam excited by electrostatic actuation. To do the analysis, we first modeled nonlocal and surface effects based on Eringen's non-local elastic theory and surface elastic theory as proposed by Gurtin and Murdoch, respectively. Subsequently, we obtained the static and dynamic modal equations by Galerkin's approach after assuming the solution based on single exact mode shape obtained by considering surface and nonlocal effects. Based on the static analysis, we analyzed the influence of surface and nonlocal effects on the pull-in voltage. We found that both surface as well nonlocal effects tend to increase the pull-in voltage effectively. To do the dynamic analysis, we solved the governing equation using the method of multiple scale. After validating the approach with numerical simulation, we analyzed frequency response of linear as well as nonlinear system. We found that resonance frequency of linear nanobeam increases with the increase in surface and nonlocal effects mainly due to increase in overall stiffness of the beam. On analyzing the response of nonlinear system of vibrations for a fixed excitation voltage, it reduced due to surface as well as nonlocal effects. Additionally, we found that while the nature of nonlinearity remained unchanged due to increase in surface effect, nonlocal effect changed the nonlinearity from hardening to softening when it was increased beyond a critical point. Therefore, it is concluded that surface and nonlocal effects modify the static and dynamic characteristics of nanobeams effectively.

Acknowledgement

This research is supported in part by the Council of Scientific and Industrial Research (CSIR), India (22(0696)/15/EMR-II).

Appendix A

$J_1 = \int_0^1 \phi(x)\,dx$, $J_2 = \int_0^1 (\phi(x))^2\,dx$, $J_3 = \int_0^1 \phi(x)\,\frac{d^6}{dx^6}\phi(x)\,dx$, $J_4 = \int_0^1 \phi(x)\,\frac{d^4}{dx^4}\phi(x)\,dx$,
$J_5 = \int_0^1 \phi(x)\,\frac{d^2}{dx^2}\phi(x)\,dx$, $J_6 = \int_0^1 (\phi(x))^2\,\frac{d^2}{dx^2}\phi(x)\,dx$, $J_7 = \int_0^1 (\phi(x))^2\,\frac{d^6}{dx^6}\phi(x)\,dx$,
$J_8 = \int_0^1 (\phi(x))^3\,dx$, $J_9 = \int_0^1 (\phi(x))^2\,\frac{d^4}{dx^4}\phi(x)\,dx$, $J_{10} = \int_0^1 \phi(x)\left(\frac{d}{dx}\phi(x)\right)^2 dx$,
$J_{11} = \int_0^1 (\phi(x))^3\,\frac{d^2}{dx^2}\phi(x)\,dx$, $J_{12} = \int_0^1 (\phi(x))^3\,\frac{d^4}{dx^4}\phi(x)\,dx$, $J_{14} = \int_0^1 (\phi(x))^3\,\frac{d^6}{dx^6}\phi(x)\,dx$,
$J_{13} = \int_0^1 \phi(x)\left(\frac{d}{dx}\phi(x)\right)^2 \frac{d^2}{dx^2}\phi(x)\,dx$, $J_{15} = \int_0^1 \phi(x)\left(\frac{d}{dx}\phi(x)\right)^2 \frac{d^4}{dx^4}\phi(x)\,dx$,
$J_{16} = \int_0^1 (\phi(x))^2\left(\frac{d}{dx}\phi(x)\right)^2 dx$, $J_{17} = \int_0^1 (\phi(x))^4\,dx$, $J_{18} = \int_0^1 (\phi(x))^4\,\frac{d^4}{dx^4}\phi(x)\,dx$,
$J_{19} = \int_0^1 (\phi(x))^2\left(\frac{d}{dx}\phi(x)\right)^2 \frac{d^4}{dx^4}\phi(x)\,dx$, $J_{20} = \int_0^1 (\phi(x))^2\left(\frac{d}{dx}\phi(x)\right)^2 \frac{d^2}{dx^2}\phi(x)\,dx$,
$J_{21} = \int_0^1 (\phi(x))^4\,\frac{d^6}{dx^6}\phi(x)\,dx$, $J_{22} = \int_0^1 (\phi(x))^4\,\frac{d^2}{dx^2}\phi(x)\,dx$, $J_{23} = \int_0^1 (\phi(x))^5\,\frac{d^4}{dx^4}\phi(x)\,dx$,
$J_{24} = \int_0^1 (\phi(x))^5\,\frac{d^6}{dx^6}\phi(x)\,dx$, $J_{25} = \int_0^1 (\phi(x))^5\,\frac{d^2}{dx^2}\phi(x)\,dx$,
$J_{26} = \int_0^1 (\phi(x))^3\left(\frac{d}{dx}\phi(x)\right)^2 \frac{d^4}{dx^4}\phi(x)\,dx$, $J_{27} = \int_0^1 (\phi(x))^3\left(\frac{d}{dx}\phi(x)\right)^2 \frac{d^2}{dx^2}\phi(x)\,dx$,
$J_{28} = \int_0^1 (\phi(x))^4\left(\frac{d}{dx}\phi(x)\right)^2 \frac{d^4}{dx^4}\phi(x)\,dx$, $J_{29} = \int_0^1 (\phi(x))^4\left(\frac{d}{dx}\phi(x)\right)^2 \frac{d^2}{dx^2}\phi(x)\,dx$,
$J_{30} = \int_0^1 (\phi(x))^5\left(\frac{d}{dx}\phi(x)\right)^2 \frac{d^2}{dx^2}\phi(x)\,dx$, $J_{31} = \int_0^1 (\phi(x))^5\left(\frac{d}{dx}\phi(x)\right)^2 \frac{d^4}{dx^4}\phi(x)\,dx$,
$J_{32} = \int_0^1 (\phi(x))^6\,\frac{d^2}{dx^2}\phi(x)\,dx$, $J_{33} = \int_0^1 (\phi(x))^6\,\frac{d^4}{dx^4}\phi(x)\,dx$, $J_{34} = \int_0^1 (\phi(x))^6\,\frac{d^6}{dx^6}\phi(x)\,dx$,
$J_{35} = \int_0^1 (\phi(x))^6\left(\frac{d}{dx}\phi(x)\right)^2 \frac{d^2}{dx^2}\phi(x)\,dx$, $J_{36} = \int_0^1 (\phi(x))^6\left(\frac{d}{dx}\phi(x)\right)^2 \frac{d^4}{dx^4}\phi(x)\,dx$,
$J_{37} = \int_0^1 (\phi(x))^3\left(\frac{d}{dx}\phi(x)\right)^2 dx$, $J_{38} = \int_0^1 (\phi(x))^5\,dx$, $J_{39} = \int_0^1 (\phi(x))^6\,dx$,
$J_{40} = \int_0^1 (\phi(x))^7\,dx$, $J_{41} = \int_0^1 \phi(x)\left(\frac{d^2}{dx^2}\phi(x)\right)^3 dx$, $J_{43} = \int_0^1 \left(\frac{d^2}{dx^2}\phi(x)\right)^3 (\phi(x))^2\,dx$
$J_{42} = \int_0^1 \left(\frac{d^2}{dx^2}\phi(x)\right)\phi(x)\left(\frac{d}{dx}\phi(x)\right)\frac{d^3}{dx^3}\phi(x)\,dx$, $J_{45} = \int_0^1 \left(\frac{d^2}{dx^2}\phi(x)\right)^3 (\phi(x))^3\,dx$
$J_{44} = \int_0^1 \left(\frac{d^2}{dx^2}\phi(x)\right)(\phi(x))^2\left(\frac{d}{dx}\phi(x)\right)\frac{d^3}{dx^3}\phi(x)\,dx$, $J_{47} = \int_0^1 \left(\frac{d^2}{dx^2}\phi(x)\right)^3 (\phi(x))^4\,dx$,
$J_{46} = \int_0^1 \left(\frac{d^2}{dx^2}\phi(x)\right)(\phi(x))^3\left(\frac{d}{dx}\phi(x)\right)\frac{d^3}{dx^3}\phi(x)\,dx$, $J_{49} = \int_0^1 \left(\frac{d^2}{dx^2}\phi(x)\right)^3 (\phi(x))^5\,dx$,
$J_{48} = \int_0^1 \left(\frac{d^2}{dx^2}\phi(x)\right)(\phi(x))^4\left(\frac{d}{dx}\phi(x)\right)\frac{d^3}{dx^3}\phi(x)\,dx$, $J_{51} = \int_0^1 \left(\frac{d^2}{dx^2}\phi(x)\right)^3 (\phi(x))^6\,dx$,
$J_{50} = \int_0^1 \left(\frac{d^2}{dx^2}\phi(x)\right)(\phi(x))^5\left(\frac{d}{dx}\phi(x)\right)\frac{d^3}{dx^3}\phi(x)\,dx$,
$J_{52} = \int_0^1 \left(\frac{d^2}{dx^2}\phi(x)\right)(\phi(x))^6\left(\frac{d}{dx}\phi(x)\right)\frac{d^3}{dx^3}\phi(x)\,dx$.

References

[1] S. C. Pradhan, M. T, Small scale effect on vibration analysis of single-walled carbon nanotubes embedded in an elastic medium using nonlocal elasticity theory, J. of Appl. Phys. 105 (2009) 124306.

[2] T. Murmu, S. Adhikari, Nonlocal frequency analysis of nanoscale biosensors, Sensors and Actuators A 173 (2012) 41–48.

[3] J. Schoebel, T. Buck, M. Reimann, M. Ulm, M. Schneider, A. Jourdain, G. J. Carchon, H. A. Tilmans, Design considerations and technology assessment of phased-array antenna systems with rf mems for automotive radar applications, IEEE Trans. Micro. Theo. Tech. 53 (2005) 1968–1975.

[4] A. E. Badri, J. K. Sinha, A. Albarbar, A typical filter design to improve the measured signals from mems accelerometer, Measurement 43 (2010) 1425–30.

[5] W. M. Zhang, H. Yan, G. Peng, Electrostatic pull-in instability in mems/nems: A review, Sensors and Actuators A: Physical 214 (2014) 187–218.

[6] J. S. Duan, R. A. Rach, A pull-in parameter analysis for the cantilever nems actuator model including surface energy, fringing field and casimir effects, International Journal of Solids and Structures 50 (2013) 3511–3518.

[7] S. D. Vishwakarma, A. K. Pandey, J. M. Parpia, D. R. Southworth, H. G. Craighead, R. Pratap, Evaluation of mode dependent fluid damping in a high frequency drumhead microresonator, IEEE J. of Microelectromech Sys. 22 (1) (2014) 334–336.

[8] M. S. Fakhrabadia, K. P. K., A. Rastgoo, M. T. Ahmadian, Molecular dynamics simulation of pull-in phenomena in carbon nanotubes with stone-wales defects, Solid State Commun. 157 (2013) 38–44.

[9] M. S. Fakhrabadia, A. Rastgoo, M. T. Ahmadian, Pull-in behaviors of carbon nanotubes with vacancy defects and residual stresses, J. of Comput. and Theor. Nanos. 11 (2014) 153–159.

[10] M. S. Fakhrabadia, A. Rastgoo, M. T. Ahmadian, On the pull-in instability of double-walled carbon nanotube-based nano electromechanical systems with cross-linked walls, Fuller. Nanotub. Car. N. 23 (2015) 300–314.

[11] M. S. Fakhrabadia, A. Rastgoo, M. T. Ahmadian, Size-dependent instability of carbon nanotubes under electrostatic actuation using nonlocal elasticity, Int. J. Mech. Scns. 80 (2014) 144–152.

[12] P. Malekzadeh, M. Shojaee, Surface and nonlocal effects on the nonlinear free vibration of non-uniform nanobeams, Compos. Part B - Eng. 52 (2013) 84–92.

[13] J. Peddieson, G. R. Buchanan, R. P. McNitt, Application of nonlocal continuum models to nanotechnology, Int. J. Eng. Sci. 41 (2003) 305–12.

[14] A. C. Eringen, D. G. B. Edelen, On nonlocal elasticity, Int. J. Eng. Sci. 10 (1972) 233–48.

[15] A. C. Eringen, Nonlocal continuum field theories, Springer, New York, 2002.

[16] R. Dingreville, J. Qu, M. Cherkaoui, Surface free energy and its effects on the elastic behavior of nano-sized particles, wires and films, J. Mech. Phys. Solids 53 (2005) 1827–54.

[17] M. E. Gurtin, I. Murdoch, A continuum theory of elastic material surface, Arch. Rat. Mech. Anal 57 (1975) 291–323.

[18] R. E. Miller, V. B. Shenoy, Size-dependent elastic properties of nanosized structural elements, Nanotechnology 11 (2000) 139–47.

[19] J. He, C. M. Lilley, Surface effect on the elastic behaviour of static bending nanowires, Nano Lett. 8 (2008) 1798.

[20] J. He, C. M. Lilley, Surface effect on bending resonance of nanowires with different boundary conditions, Appl. Phys. Lett. 93 (2008) 263108.

[21] H. Sheng, H. Li, P. Lu, H. Xu, Free vibration analysis for micro-structures used in mems considering surface effects, J. Sound Vib. 329 (2010) 236–46.

[22] S. Abbasion, A. Rafsanjani, R. Avazmohammadi, A. Farshidianfar, Free vibration of microscaled timoshenko beams, Appl. Phys. Lett. 95 (2009) 143122.

[23] H. S. M. Gheshlaghi, B., Surface effects on nonlinear free vibration of nanobeams, Compos. Part B - Eng. 42 (2011) 934–7.

[24] S. Hosseini-Hashemi, R. Nazemnezhad, An analytical study on the nonlinear free vibration of functionally graded nanobeams incorporating surface effects, Compos. Part B - Eng. 52 (2013) 199–206.

[25] P. Lu, L. He, H. Lee, C. Lu, Thin plate theory including surface effects, Int. J. Solids Struct. 43 (2006) 4631–4647.

[26] C. Liu, R. K. N. D. Rajapakse, Continuum models incorporating surface energy for static and dynamic response of nanoscale beams, IEEE T. Nanotechnology 9 (2010) 422–431.

[27] K. M. Hu, W. M. Zhang, Z. Y. Zhong, Z. K. Peng, G. Meng, Effect of surface layer thickness on buckling and vibration of nonlocal nanowires, Phys. Lett. A 378 (2014) 650–654.

[28] K. M. Hu, W. M. Zhang, Z. K. Peng, G. Meng, Transverse vibrations of mixed-mode cracked nanobeams with surface effect, J. Vib. Acoust. 138 (2016) 011020–1.

[29] C. M. Wang, Y. Y. Zhang, X. Q. He, Vibration of nonlocal timoshenko beams, Nanotechnology 18 (2007) 105401.

[30] T. Murmu, S. Adhikari, Nonlocal transverse vibration of double-nanobeam systems, J. Appl. Phys. 108 (2010) 083514.

[31] J. N. Reddy, Nonlocal nonlinear formulations for bending of classical and shear deformation theories of beams and plates, Int. J. Eng. Sci. 48 (2010) 1507–18.

[32] L. L. Ke, Y. S. Wang, Z. D. Wang, Nonlinear vibration of the piezoelectric nanobeams based on the nonlocal theory, Compos. Struct. 94 (2012) 2038–47.

[33] K. M. Hu, W. M. Zhang, X. J. Dong, Z. K. Peng, G. Meng., Scale effect on tension-induced intermodal coupling in nanomechanical resonators, J. of Vib. Acoust. 137 (2) (2015) 021008–14.

[34] H. L. Lee, W. J. Chang, Surface effects on frequency analysis of nanotubes using nonlocal timoshenko beam theory, J. Appl. Phys. 108 (2010) 093501–3.

[35] H. L. Lee, W. J. Chang, Surface and small-scale effects on vibration analysis of a nonuniform nanocantilever beam, Physica E 43 (2010) 466–9.

[36] R. Nazemnezhad, M. Salimi, An analytical study on the nonlinear free vibration of nanoscale beams incorporating surface density effects, Compos. Part B - Eng. 43 (2012) 2893–2897.

[37] R. Ardito, C. Comi, Nonlocal thermoelastic damping in micromechanical resonators, J. Eng. Mech. 135 (2009) 214–220.

[38] Y. Lei, S. Adhikari, M. I. Friswell, Vibration of nonlocal kelvin-voigt viscoelastic damped timoshenko beams, Int. J. Eng. Sci. 67 (2013) 1–13.

[39] I. Dumitru, M. Israel, W. Martin, Reduced order model analysis of frequency response of alternating current near half natural frequency electrostatically actuated mems cantilevers, J. Comp. Non. Dyn. 8 (2013) 031011–031015.

[40] A. H. Nayfeh, M. I. Younis, E. M. Abdel-Rahman, Dynamic pull-in phenomenon in mems resonators, Nonlinear Dyn. 48 (2007) 153–163.

[41] A. K. Pandey, Effect of coupled modes on pull-in voltage and frequency tuning of a nems device, J. Micromech. and Microengg. 23 (2013) 085015–085024.

[42] T. Mousavi, S. Bornassi, H. Haddadpour, The effect of small scale on the pull-in instability of nano-switches using dqm, Int. J. Solids Struct. 50 (2012) 1193–202.

[43] J. Yang, X. L. Jia, S. Kitipornchai, Pull-in instability of nano-switches using nonlocal elasticity theory, J. Phys. D: Appl. Phys. 41 (2008) 035103.

[44] A. Pasharavesh, M. T. Ahmadian, R. Moheimani, Nonlinear vibration analysis of nano to micron scale beams under electric force using nonlocal theory, in: Proc of 5th International conference on Micro- and Nanosystems, Vol. 7, 2011.

[45] P. Lu, H. P. Lee, P. Q. Zhang, Dynamic properties of flexural beams using a nonlocal elasticity model, J. Appl. Phys. 99 (2006) 073510.

[46] P. C. P. Chao, C. W. Chiu, T. H. Liu, Dc dynamic pull-in predictions for a generalized clamped-clamped micro-beam based on a continuous model and bifurcation analysis, J. Micromech. Microeng. 18 (2008) 115008.

[47] Y. Fang, L. Pu, A new approach and model for accurate determination of the dynamic pull-in parameters of microbeams actuated by a step voltage, J. Micromech. Microeng. 23 (2013) 045010.

[48] I. Kozinsky, H. W. C. Postma, I. Bargatin, M. L. Roukes, Tuning nonlinearity, dynamic range, and frequency of nanomechanical resonators, Appl. Phys. Lett. 88 (2006) 253101–3.